

<https://doi.org/10.15407/ujpe68.6.375>

A. JUMABAEV,<sup>1</sup> H. HUSHVAKTOV,<sup>1</sup> B. KHUDAYKULOV,<sup>1</sup> A. ABSANOV,<sup>1</sup>  
M. ONUK,<sup>2</sup> I. DOROSHENKO,<sup>2</sup> L. BULAVIN<sup>2</sup>

<sup>1</sup> Sharof Rashidov Samarkand State University

(15, University Blvd., Samarkand 703004, Uzbekistan; e-mail: jumabaev2@rambler.ru)

<sup>2</sup> Taras Shevchenko National University of Kyiv

(64/13, Volodymyrska Str., Kyiv 01601, Ukraine)

---

## FORMATION OF HYDROGEN BONDS AND VIBRATIONAL PROCESSES IN DIMETHYL SULFOXIDE AND ITS AQUEOUS SOLUTIONS: RAMAN SPECTROSCOPY AND AB INITIO CALCULATIONS

---

*The intermolecular interaction in dimethyl sulfoxide (DMSO), which is a strong solvent, and its manifestation in vibrational spectra are studied by means of Raman spectroscopy and ab initio calculations. The optimal structure and vibrational spectra of DMSO monomer, dimer, and trimer, as well as complexes of DMSO with water molecules, are calculated, and the potential energy distribution (PED) analysis is carried out. In the Raman spectra of DMSO and its water solutions, a red shift of the S=O stretching band due to the conventional hydrogen bonding and a blue shift of the C-H stretching band due to non-classical hydrogen bonding are detected. The MEP surfaces (changes in the charge distribution) of DMSO monomer, dimer, and DMSO-water cluster are plotted.*

*Keywords:* dimethyl sulfoxide, Raman spectroscopy, ab initio calculations, hydrogen bonding, cluster.

### 1. Introduction

Raman spectroscopy is widely used to study the structure of molecules, intermolecular and intramolecular H-bonds, interactions between a solute and a solvent, *etc.* [1–7]. Understanding the structure and intermolecular interactions in the liquid phase is im-

portant for the detailed study of the microscopic aspects of the solution formation [8].

Dimethyl sulfoxide ((CH<sub>3</sub>)<sub>2</sub>SO) is a good inorganic solvent, which is widely used in pharmaceuticals due to its rapid penetration through human skin [9]. Despite the fact that the internal structure of DMSO and the intermolecular interactions in it have been studied in various ways, the interactions between DMSO molecules in the liquid state have not been fully explained till now [10]. Since DMSO properties are similar to those of water, it is often used as a solvent in experiments and processes involving water [11]. In biology and medical applications, DMSO is widely used due to its high crystallization temperature in the aqueous medium and other properties related to its ability to form hydrogen bonds [12, 13].

---

Citation: Jumabaev A., Hushvaktov H., Khudaykulov B., Absanov A., Onuk M., Doroshenko I., Bulavin L. Formation of hydrogen bonds and vibrational processes in dimethyl sulfoxide and its aqueous solutions: Raman spectroscopy and ab initio calculations. *Ukr. J. Phys.* **68**, No. 6, 375 (2023). <https://doi.org/10.15407/ujpe68.6.375>.

Цитування: Жумабаєв А., Хушвактов Х., Абсанов А., Онук М., Дорошенко І., Булавін Л. Утворення водневих зв'язків та коливальні процеси в диметилсульфоксиді та його водних розчинах: раманівська спектроскопія та *ab initio* розрахунки. *Укр. фіз. журн.* **68**, № 6, 375 (2023).

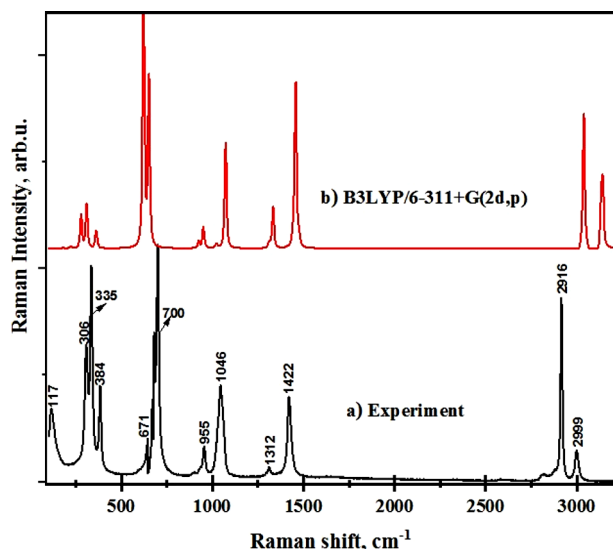


Fig. 1. Raman spectra of pure DMSO: experiment (a), calculation (b)

According to ab initio calculations, the hydration of DMSO in an aqueous environment occurs, leading to the red shift of the S=O stretching vibration frequency and the blue shift of the C–H stretching vibration frequency [14]. E.V. Ivanov and others mentioned that weak C–H...O=S hydrogen bonds are formed in liquid DMSO, and, in DMSO-water complexes, stronger hydrogen bonds are formed, as compared to water-water associates [11]. B. Yang and others also studied the aqueous solutions of DMSO with different concentrations [15]. They observed a shift of the O–H stretching band of water to the low-frequency side with increasing the concentration. When the proportion of DMSO is 0.6 mol, a red shift of S=O stretching vibrations and a blue shift of C–H stretching vibration are observed [15]. The Raman spectra of neat DMSO and its binary mixtures with water and methanol in both  $\nu(\text{S}=\text{O})$  and  $\nu(\text{C}-\text{H})$  regions were studied in [16]. The significant blue shift of the C–H frequency due to C–H...O hydrogen bonding was also obtained in the case of both solvents [16]. In our previous work [17], dimethyl sulfoxide was studied experimentally and with use of the semiempirical (quasi-empirical) MINDO/3 method of calculations. The high possibility of dipole-dipole interactions between DMSO molecules in aqueous and other binary solutions was shown. In [5], it was found that the non-classical hydrogen bond can be formed not only via the C–H bond, but also through  $\pi$  elec-

trons in aromatic rings. In the study of intermolecular interactions, an important role is played by determining the contribution of each vibrational frequency, explaining non-classical hydrogen bonds by changes in bond lengths and in the charge distribution.

## 2. Experimental and Theoretical Methods

An experimental investigation was carried out using an InViaRaman spectrometer with a constant of the diffraction grating to be 1200 lines/mm. The integration time is 10 s, and the resolution is  $0.5 \text{ cm}^{-1}$ . A Spectrum Stabilized Laser Module with a wavelength of 785 nm and a power of 100 mW was used as an excitation source. Spectra were recorded using a Renishaw CCD Camera detector with a 20x focus. The samples were obtained by dissolving DMSO in water.

Since the d orbitals in the sulfur atom are involved in the S=O double bond, it is necessary to choose a suitable basis set in order to adequately describe the electronic structure of the molecule in these orbitals. To calculate the structure of the DMSO molecule and its vibration frequencies, we used the basis set 6-311 + G(2d,p) (in the Gaussian 09 program, DFT method) based on f functions on the sulfur atom and diffuse s and p functions on the sulfur and oxygen atoms [18]. The PED analysis was performed using VEDA 4.0 software.

## 3. Results and Discussions

### 3.1. Vibrational frequencies analysis

The development of a computer technology makes it possible to compare the results of experiments with the results of calculations, as well as to determine physical quantities that cannot be obtained experimentally. We must first determine the compatibility of experimental data and calculations before evaluating such parameters. Figure 1, a shows an experimentally registered Raman spectrum of liquid DMSO, which is rather complex and has multiple vibrational maxima. The Raman spectrum of pure DMSO was compared to the spectrum calculated in the B3LYP/6-311 + G(2d,p) approximation (Fig. 1, b). It can be seen from Fig. 1 that the experimental and calculated Raman spectra of DMSO are in a good agreement. In addition, a potential energy distribution (PED) analysis was performed for the DMSO molecule, and the theoretically determined frequencies were compared with the experimental values (Table 1).

Table 1. Raman frequencies and assignments of normal modes of DMSO

| Modes | Observed frequency, $\text{cm}^{-1}$ | Calculated frequency (DFT), $\text{cm}^{-1}$ | Exp./Calc. | Potential energy distribution                                     |
|-------|--------------------------------------|--|------------|---|
| 1     |                                      | 3143   |            | CH <sub>3</sub> asym. str. (98%)                                  |
| 2     |                                      | 3142   |            | CH <sub>3</sub> sym. str. (22%), CH <sub>3</sub> asym. str. (75%) |
| 3     |                                      | 3135   |            | CH <sub>3</sub> asym. str. (98%)                                  |
| 4     | 2999                                 | 3130   | 0.96       | CH <sub>3</sub> sym. str. (98%)                                   |
| 5     | 2916                                 | 3038   | 0.96       | CH <sub>3</sub> sym. str. (99%)                                   |
| 6     |                                      | 3035   |            | CH <sub>3</sub> sym. str. (99%)                                   |
| 7     |                                      | 1476   |            | CH <sub>3</sub> asym. bend. (72%), C–S–C asym. tor. (23%)         |
| 8     |                                      | 1457   |            | CH <sub>3</sub> asym. bend. (71%), C–S–C asym. tor. (20%)         |
| 9     |                                      | 1455   |            | CH <sub>3</sub> sym. bend. (71%), C–S–C tor. (20%)                |
| 10    |                                      | 1441   |            | CH <sub>3</sub> asym. bend. (77%), C–S–C asym. tor. (20%)         |
| 11    | 1422                                 | 1333   | 1.07       | CH <sub>3</sub> sym. bend. (94%)                                  |
| 12    | 1312                                 | 1312   | 1.00       | CH <sub>3</sub> sym. bend. (98%)                                  |
| 13    |                                      | 1072   |            | S=O str. (83%), CSC asym. tor. (10%)                              |
| 14    |                                      | 1022   |            | CH <sub>3</sub> asym. bend. (22%), C–S–C asym. tor. (60%)         |
| 15    | 1046                                 | 951  | 1.10       | CH <sub>3</sub> sym. bend. (19%), C–S–C tor. (55%)                |
| 16    |                                      | 925  |            | CH <sub>3</sub> sym. bend. (18%), C–S–C tor. (56%)                |
| 17    | 955                                  | 891  | 1.07       | CH <sub>3</sub> asym. bend. (22%), C–S–C tor. (68%)               |
| 18    | 700                                  | 652  | 1.07       | S–C str. (90%)  |
| 19    | 671                                  | 623  | 1.08       | S–C str. (95%)  |
| 20    | 384                                  | 363  | 1.06       | C–S–C asym. bend. (11%), C–C–S out bend. (75%)                    |
| 21    | 335                                  | 310  | 1.08       | O–S–C bend. (89%)   |
| 22    | 306                                  | 280  | 1.09       | C–S–C bend. (80%), C–C–S out bend. (11%)                          |
| 23    |                                      | 223  |            | C–S–C asym. tor. (98%)  |
| 24    | 117                                  | 180  | 0.65       | C–S–C tor. (94%)  |

Abbreviations: str., stretching; bend., bending; tor., torsion; sym., symmetric; asym., asymmetric; out, out of plane

In the experiment, the C–H symmetric stretching vibrations are located at  $2999 \text{ cm}^{-1}$  and  $2916 \text{ cm}^{-1}$ . In the theoretically calculated spectrum, these values are, respectively,  $3130$  and  $3038 \text{ cm}^{-1}$ , which is consistent with an error of 4%. The band at  $1422 \text{ cm}^{-1}$  corresponds to the C–H symmetric stretching vibrations. In calculations, this value is  $1333 \text{ cm}^{-1}$  and differs by 7% from the experimental one. The wavenumber of  $1046 \text{ cm}^{-1}$  corresponds to the combination of S=O stretching, CH symmetric stretching, and C–S–C torsion vibrations, and the calculated value is  $951 \text{ cm}^{-1}$  and differs from the experimental value by 10%. A combination of CH asymmetric stretching and C–S–C torsion vibrations is manifested at  $955 \text{ cm}^{-1}$ . The corresponding calculated value is  $891 \text{ cm}^{-1}$  and differs from the experimental result by 7%. The other six bands are assigned to vibrations involving sulfur, carbon, and oxygen atoms and differ by 10% from the experimental results. However, the wave number of  $117 \text{ cm}^{-1}$  corre-

sponding to C–S–C torsion vibrations obtained in the experiment is significantly different from the calculated value. In general, the experimentally obtained Raman spectrum of DMSO agrees with the calculated frequencies within 10%.

### 3.2. Geometry optimization

Figure 2 presents the calculated (DFT) optimal geometry of DMSO monomer, dimer, and trimer. The monomer of DMSO (Fig. 2, *a*) has a dipole moment of 4.15 D and  $C_s$  symmetry. Figure 2, *b* shows a dimer of DMSO, and the formation of the dimer results in a closed structure connected by 4 hydrogen bonds. Two of these bonds are formed by O16, H13, and H19 atoms of DMSO. All bond lengths are equal to  $2.4 \text{ \AA}$ , and the complex formation energy is 5.98 kcal/mol. The dipole moment of the dimer is significantly reduced, as compared to the monomer – 0.0008 D. This is related to the orientation of the molecule, which means that the dimer

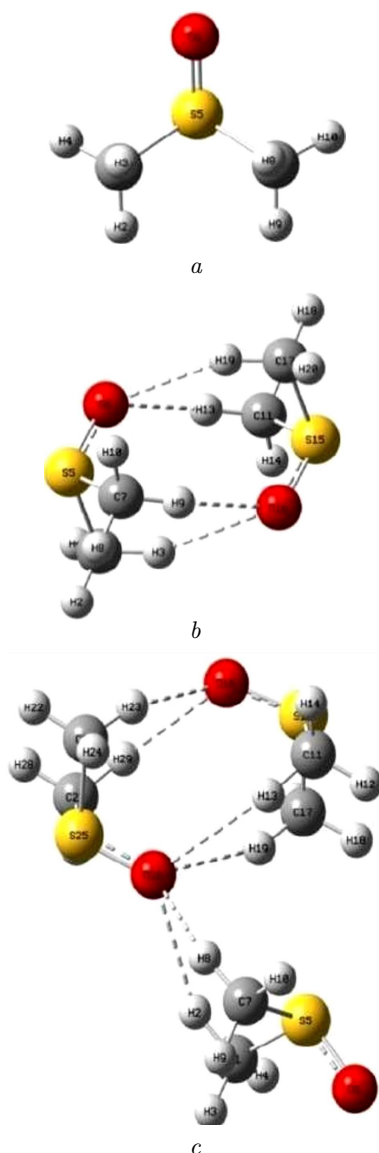


**Fig. 2.** Optimal geometry of DMSO monomer (a), dimer (b), and trimer (c)

molecule is symmetrically located (has  $C_{2h}$  symmetry). The trimer has  $C_s$  symmetry and the energy of trimer formation is 8.91 kcal/mol (Fig. 2, c). Another molecule is connected by two H-bonds to the cyclic chain in the dimer through six H-bonds in the trimer. H23 and H29 are H-bonded to atoms O16, with all bond lengths 2.37 Å. All mentioned bonds are weak hydrogen bonds in the form of  $C-H\cdots O$ , and such bonds are called non-classical hydrogen bonds in the literature [19].

### 3.3. Interactions of DMSO in aqueous media

According to the Pauli principle, the classical definition of H-bonding is that the H atom located between two atoms with high electronegativity is strongly (covalently) bonded to one of them and interacts electrostatically with the other one. This interaction is called hydrogen bonding. In the  $H-A\cdots B$  form, the  $A-H$  distance increases, resulting in a red-shift in the  $A-H$  stretching vibrational frequency. However, in 1964, Suttor studied the  $C-H\cdots B$  interaction in crystals ( $\pi$  electrons can be substituted for B as a proton acceptor). In such a bond, the  $C-H$  distance decreases, resulting in a blue shift in the frequency of the  $C-H$  stretching vibrations. For this reason, it does not correspond to the classical definition of H-bonding. It is also weak in terms of energy. This phenomenon is called anti-H-bonding or non-classical H-bonding [19]. Non-classical H-bonds in DMSO/water systems explains the shift of  $C-H$  stretching vibration band toward higher frequencies [11–13]. We also use Raman spectroscopy and ab initio calculations to demonstrate the formation of conventional and non-classical hydrogen bonds in DMSO and its aqueous solution by red-shifting the  $S=O$  stretching vibration frequency and blue-shifting the  $C-H$  stretching vibration frequency, and by changing the  $C-H$  bond length. In order to further confirm the presence of non-classical hydrogen bonds between DMSO molecules, experiments were conducted in the aqueous medium with DMSO. In this case, we isolated only the  $S=O$  and  $C-H$  bands involved in conventional and non-classical hydrogen bonds from the total Raman spectra of DMSO, pure and in an aqueous medium.

The Raman spectra of pure DMSO and its aqueous solution in the region of  $S=O$  and  $C-H$  stretching vibrations are presented in Fig. 3. It can be seen that, in pure DMSO, the  $S=O$  band is located at  $1046\text{ cm}^{-1}$ . In the aqueous solution, it is shifted toward lower frequencies by  $9\text{ cm}^{-1}$ . In our opinion, the reason for such a shift is the conventional hydrogen bond formed by  $S=O$  bond. The  $C-H$  stretching bands at  $2916$  and  $2999\text{ cm}^{-1}$  in pure DMSO are shifted to higher frequencies in aqueous media. Such a shift is due to the non-classical hydrogen bond formed by  $C-H$  bond. To confirm this idea, ab initio calculations were carried out. Figure 4, a shows the calculated structures of a heterodimer of DMSO with one

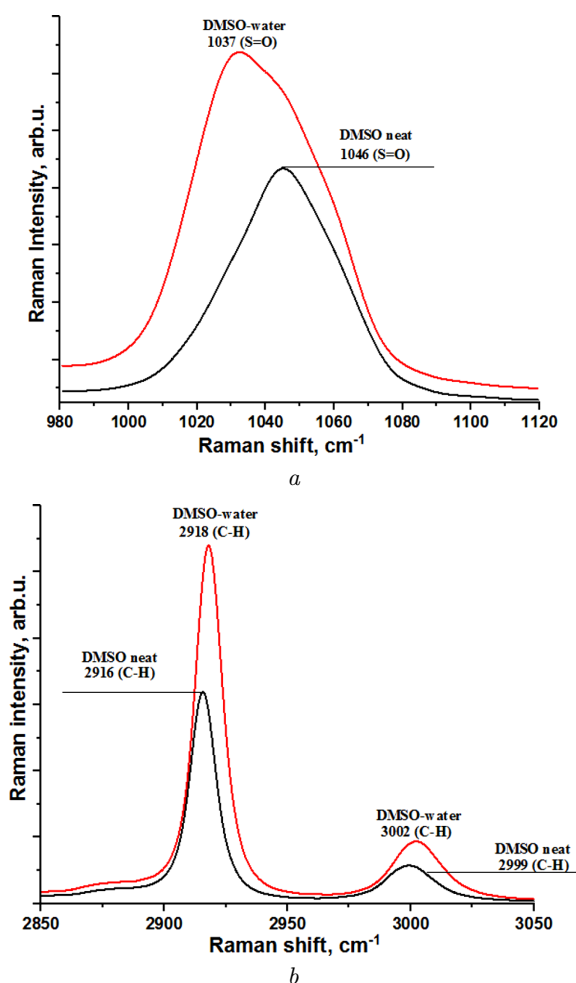


**Fig. 3.** Raman spectra of pure DMSO (a) and its aqueous solution (b) in the region of S=O and C-H stretching vibrations

water molecule, and there is an H-bond between the O6 atom of DMSO and the H12 atom of water with a bond energy of 2.12 kcal/mol. When the number of water molecules is increased by one (Fig. 4, b), the number of these bonds reaches three. The energy of complex formation is 4.53 kcal/mol. In this case, two bonds are in O-H...O form, and the third one is a non-classical C-H...O bond with the hydrogen atom of DMSO molecule, and the blue shift observed in Fig. 4, a is due to this bond. Figure 4, c shows the complex of one DMSO and three water molecules. There are five H-bonds with an energy of 6.75 kcal/mol. Two of these bonds are C-H...O with bond lengths of 2.37 and 2.40 Å, other bonds are formed as O-H...O bonds with a bond length of about

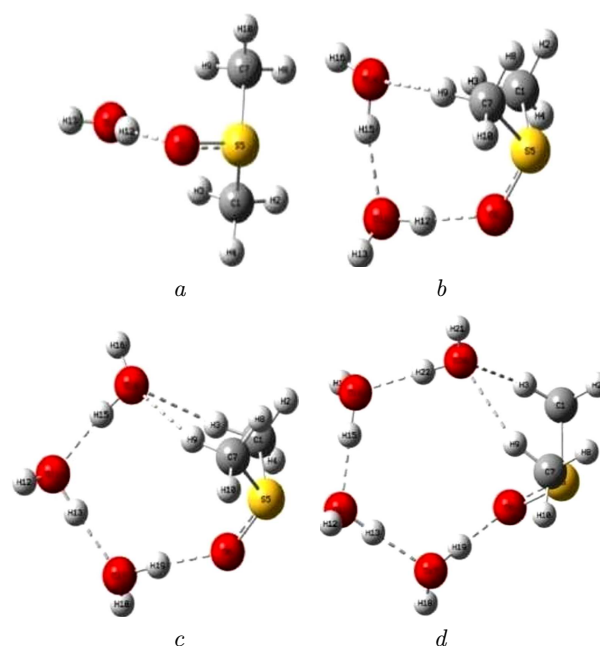


**Fig. 4.** Complexes formed by DMSO with water molecules; DMSO + 1W (a), DMSO + 2W (b), DMSO + 3W (c), DMSO + 4W (W-water) (d)

1.73 Å and are relatively strong. In the case where the number of water molecules is four, the energy of the complex is 9.07 kcal/mol. Here, the number of H-bonds is six, two of which are of the C-H...O type, as mentioned above, and the rest are formed as O-H...O. So, one can draw the conclusion that the oxygen atom of a DMSO molecule is connected through a normal hydrogen bond. Hydrogen atoms of two methyl groups are connected through non-classical H-bonds. Thus, the results of calculations confirm that the blue shift of the vibrational band occurs due to the C-H...O bonds formation, and the red shift – due to S=O...H bonds.

### 3.4. Changes in S=O and C-H bond lengths due to the hydrogen bonding

In a conventional hydrogen bond, the frequency of stretching vibrations decreases, and the length of the stretching bond increases. In a non-classical hydrogen bonding, the stretching vibration frequency should increase, and the length of the stretching bond should decrease. Therefore, using ab initio calculations, the changes in S=O and C-H bond lengths due to the

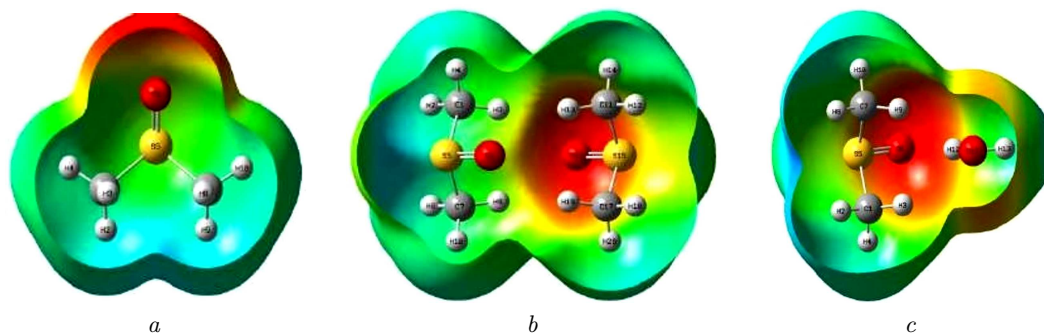


**Fig. 5.** MEP energy surfaces of a DMSO monomer, DMSO dimer, and DMSO + water dimer

hydrogen bonding in pure DMSO and clusters formed with water molecules were studied.

The length of the S=O stretching bond in a DMSO monomer molecule is 1.50145 Å, and, in the dimer and trimer complexes, this distance is extended due to the conventional hydrogen bonding (Table 2). This distance is longer for DMSO-water<sub>n</sub> (*n* = 1–4) complexes compared to a DMSO monomer. The C–H bond length is 1.09007 Å (C1–

H3) and 1.09081 Å (C7–H9) for a DMSO monomer molecule. In dimer and trimer complexes, this distance is reduced due to the non-classical hydrogen bonding. For DMSO-water<sub>n</sub> (*n* = 1–4) complexes, the C–H bond length was also reduced compared to a DMSO monomer. This confirms that, indeed, DMSO (both in the pure form and in aqueous media) contains non-classical hydrogen bonds along with conventional hydrogen bonds.

### 3.5. MEP surfaces

A molecular electro-potential (MEP) surface (electrostatic potential energy map) characterizes the 3D charge distribution of a molecule. Figure 5 shows the MEP surfaces for a DMSO molecule, DMSO dimer, and complex of DMSO and water molecules. These surfaces are represented in different colors depending on the potential level. The order of increasing the electrostatic potential is shown in orange < yellow < green < blue. It can be seen from Fig. 5 that the surface around the S=O bond is in orange color, i.e., it has the lowest potential, and C–H is in blue color, which means that it has the greatest electrostatic potential. These parts are also considered to be active in the hydrogen bonding. It can be seen from the figure that the color (MEP surface) is changed, when DMSO passes from a monomer to a dimer and a DMSO-water cluster, which means that the charge distribution is also changed. Another main reason for the formation of a non-classical hydrogen bond can be a change in this charge distribution.

According to the formula

$$\nu = \frac{1}{2\pi} \sqrt{\frac{k}{m}},$$

the vibrational frequency is inversely proportional to the square root of the atomic mass. So, in a con-

**Table 2.** Distances between atoms (Å) in S=O and C–H bonds in pure DMSO and its aqueous solution

| Bonds          | S=O bonds   | C–H bonds  |
|----------------|---|--|
| DMSO monomer   | 1.50145(S=O6)   | 1.09070 (C1–H3)<br>1.09081(C7–H9)  |
| DMSO dimer     | 1.51301 (S5=O6)<br>1.51291 (S15=O16)                      | 1.09029 (C11–H13)<br>1.09028 (C12–H19)<br>1.09028 (C1–H3)<br>1.09030 (C7–H9)   |
| DMSO trimer    | 1.50477 (S5=O6)<br>1.51365 (S15=O16)<br>1.51886 (S25=O26) | 1.09035 (C27–H29)<br>1.09035 (C21–H23)<br>1.08981 (C11–H13)<br>1.08979 (C17–H19)<br>1.09067 (C7–H8)<br>1.09064 (C1–H2) |
| DMSO + 1 Water | 1.51609 (S5=O6)   | 1.08989 (C1–H3)<br>1.08989 (C7–H9)   |
| DMSO + 2 Water | 1.51883 (S5=O6)   | 1.09035 (C1–H3)<br>1.09004 (C7–H9)   |
| DMSO + 3 Water | 1.51803 (S5=O6)   | 1.09029 (C1–H3)<br>1.08971 (C7–H9)   |
| DMSO + 4 Water | 1.52092 (S5=O6)   | 1.09000 (C1–H3)<br>1.09039 (C7–H9)   |



ventional hydrogen bond, the frequency decreases with increasing the mass. But, this frequency also depends on the force constant  $k$ . Conventional hydrogen bonds are mainly formed by atoms with high electronegativity, while non-classical hydrogen bonds are formed by atoms with low electronegativity (for example, C). Therefore, for atoms with such low electronegativity, an increase in the frequency and a decrease in the stretching distance can be observed due to the fact that the force constant  $k$  is large.

#### 4. Conclusions

Intermolecular interactions in pure DMSO and its aqueous solutions have been studied by means of Raman spectroscopy and quantum-chemical calculations. Vibrational frequencies of DMSO are determined by the PED analysis, and the obtained values are found to be in a good agreement with the experimentally registered ones. The intermolecular interaction between DMSO molecules is manifested in Raman spectra as a red shift of the S=O stretching vibration band and a blue shift of the C-H stretching vibration band. These shifts are also observed in the spectra of aqueous solutions of DMSO. The red shift can be explained by an increase in the bond length due to the conventional hydrogen bonding formation, and a blue shift – by a decrease in the bond length due to a non-classical hydrogen bonding. During the formation of a DMSO dimer, trimer, and DMSO + water molecular clusters, a change in the charge distribution of atoms is observed. The conclusion can be drawn that non-classical hydrogen bonds can be formed due to changes in the charge distribution of atoms, and the value of the force constant is larger for atoms with low electronegativity.

1. L. Ma, H. Li, C. Wang, Y. Xu, Sh. Han. Prediction of vapor–liquid equilibria data from C–H band shifts of Raman spectra and activity coefficients at infinite dilution in some aqueous systems. *Ind. Eng. Chem. Res.* **44**, 6883 (2005).
2. V. Pogorelov, L. Bulavin, I. Doroshenko, O. Fesjun, O. Veretennikov. The structure of liquid alcohols and the temperature dependence of vibrational bandwidth. *J. Mol. Struct.* **708**, 61 (2004).
3. L. Bulavin, I. Doroshenko, O. Lizengevyich, V. Pogorelov, L. Savransky, O. Veretennikov. Raman study of molecular associations in methanol. *Proc. SPIE* **5507**, 138 (2004).
4. V. Pogorelov, A. Yevglevsky, I. Doroshenko, L. Berezovchuk, Yu. Zhovtobryuch. Nanoscale molecular clusters and vibrational relaxation in simple alcohols. *Superlattices Microstruct.* **44**, 571 (2008).
5. A. Jumabaev, B. Khudaykulov, I. Doroshenko, H. Hushvaktov, A. Absanov. Raman and ab initio study of intermolecular interactions in aniline. *Vib. Spectrosc.* **122**, 103422 (2022).
6. H. Hushvaktov, B. Khudaykulov, A. Jumabaev, I. Doroshenko, A. Absanov, G. Murodov. Study of formamide molecular clusters by Raman spectroscopy and quantum-chemical calculations. *Mol. Cryst. Liq. Cryst.* **749**, 124 (2022).
7. E.N. Kozlovskaya, G.A. Pitsevich, A.E. Malevich, O.P. Doroshenko, V.E. Pogorelov, I.Yu. Doroshenko, V. Balevicius, V. Sablinskas, A.A. Kamnev. Raman spectroscopic and theoretical study of liquid and solid water within the spectral region 1600–2300  $\text{cm}^{-1}$ . *Spectrochim. Acta A* **196**, 406 (2018).
8. B.A. Marekha, K. Sonoda, T. Uchida, T. Tokuda, A. Id-rissi, T. Takamuku. ATR-IR spectroscopic observation on intermolecular interactions in mixtures of imidazolium-based ionic liquids  $C_n\text{mimTFSA}$  ( $n = 2\text{--}12$ ) with DMSO. *J. Mol. Liq.* **232**, 431 (2017).
9. R. Thomas, C.B. Shoemaker, K. Eriks. The molecular and crystal structure of dimethyl sulfoxide. *Acta Cryst.* **21**, 12 (1966).
10. H. Torii, M. Tasumi. Raman noncoincidence effect and intermolecular interactions in liquid dimethyl sulfoxide: Simulations based on the transition dipole coupling mechanism and liquid structures derived by Monte Carlo method. *Bull. Chem. Soc. Jpn.* **68**, 128 (1995).
11. E.V. Ivanov, E.Yu. Lebedeva, V.K. Abrosimov, N.G. Ivanova. Densimetric studies of binary solutions involving  $\text{H}_2\text{O}$  or  $\text{D}_2\text{O}$  as a solute in dimethylsulfoxide at temperatures from (293.15 to 328.15) K and atmospheric pressure. *J. Solution Chem.* **41**, 1311 (2012).
12. P.P. Wiewior, H. Shirota, E. Castner. Aqueous dimethyl sulfoxide solutions: Inter- and intra-molecular dynamics. *J. Chem. Phys.* **116**, 4643 (2002).
13. Q. Zhang, X. Zhang, D.X. Zhao. Polarizable force field for water-dimethyl sulfoxide systems: II properties of mixtures by molecular dynamics simulations. *J. Mol. Liq.* **145**, 67 (2009).
14. E. Mrazkova, P. Hobza. Hydration of sulfo and methyl groups in dimethyl sulfoxide is accompanied by the formation of red-shifted hydrogen bonds and improper blue-shifted hydrogen bonds: an ab initio quantum chemical study. *J. Phys. Chem. A* **107**, 1032 (2003).
15. B. Yang, X. Cao, Ch. Wang, Sh. Wang, Ch. Sun. Investigation of hydrogen bonding in Water/DMSO binary mixtures by Raman spectroscopy. *Spectrochim. Acta A* **228**, 117704 (2020).
16. Sh. Singh, S.K. Srivastava, D.K. Singh. Raman scattering and DFT calculations used for analyzing the structural features of DMSO in water and methanol. *RSC Adv.* **3**, 4381 (2013).
17. A. Jumabaev, F.H. Tuhvatullin, U.N. Tashkenbaev, Z. Mamatov. Raman spectra of S=O vibrations of di-

methylsulphoxide in liquid state. *Proc. SPIE* **4812**, 4812 (2002).

18. M.J. Frisch, G.W. Trucks, H.B. Schlegel, G.E. Scuseria, M.A. Robb et al. *Gaussian 09*, Revision A.02.

19. S.J. Grabowski. *Hydrogen Bonding – New Insights* (Springer, 2006).

Received 11.04.23

A. Жумабаєв, Х. Хушвактов, Б. Худайкулов,  
А. Абсанов, М. Онук, І.Ю. Дорошенко, Л. Булавін

УТВОРЕННЯ ВОДНЕВИХ  
ЗВ'ЯЗКІВ ТА КОЛИВАЛЬНІ ПРОЦЕСИ  
В ДИМЕТИЛСУЛЬФОКСИДІ ТА ЙОГО ВОДНИХ  
РОЗЧИНАХ: РАМАНІВСЬКА СПЕКТРОСКОПІЯ  
ТА *AB INITIO* РОЗРАХУНКИ

Методами раманівської спектроскопії та *ab initio* розрахунків досліджено міжмолекулярну взаємодію в диметилсуль-

фоксиді (ДМСО), який є сильним розчинником, та її прояв у коливальних спектрах. Розраховано оптимальну структуру та коливальні спектри мономера, димера та тримера ДМСО, а також комплексів ДМСО з молекулами води та проведено аналіз розподілу потенціальної енергії (PED). У раманівських спектрах ДМСО та його водних розчинів було виявлено червоний зсув смуги валентних S=O коливань внаслідок утворення звичайного водневого зв'язку та синій зсув смуги валентних C–H коливань внаслідок утворення неklasичного водневого зв'язку. Побудовано поверхні MEP (зміни в розподілі заряду) мономера і димера ДМСО, а також кластера ДМСО-вода.

*Ключові слова:* диметилсульфоксид, раманівська спектроскопія, розрахунки *ab initio*, водневий зв'язок.